

Aryl Cation and Carbene Intermediates in the Photodehalogenation of Chlorophenols

Ilse Manet,^[a] Sandra Monti,^{*,[a]} Maurizio Fagnoni,^[b] Stefano Protti,^[b] and Angelo Albini^{*,[b]}

Abstract: The photochemistry of 2,6-dimethyl-4-chlorophenol (**6**) has been studied in methanol and trifluoroethanol (TFE) through product studies and transient absorption spectroscopy. Chloride loss from triplet **6** gave triplet hydroxyphenyl cation **14**, which equilibrated with triplet oxocyclohexadienylidene **15** within a few tens of nanoseconds; the cation can, however, be selectively trapped by allyltrimethylsilane ($k_{\text{ad}} = 10^8\text{--}10^9 \text{ M}^{-1} \text{ s}^{-1}$) to give a pheno-

nium ion and the allylated phenol. In neat alcohols, **14** and **15** are reduced through different mechanisms, namely by hydrogen transfer through radical cation **17** and via phenoxyl radical **16**, respectively. The mechanistic rationalization has been substantiated by the

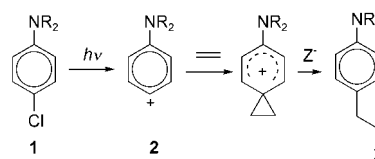
parallel study of an O-silylated derivative. The work shows that the chemistry of the highly (but selectively) reactive phenyl cation **14** can not only be discriminated from that of the likewise highly reactive carbene **15**, but also exploited for synthetically useful reactions, as in this case with alkenes. Photolysis of electron-donating substituted halobenzenes may be the method of choice for the mild generation of some classes of phenyl cations.

Keywords: aryl cations • carbenes • chlorophenols • laser flash photolysis • photochemistry

Introduction

The generation of a highly activated intermediate under mild conditions is one of the most interesting applications of photochemistry. Mostly, this principle finds application in mechanistic studies since irradiation offers a smooth way of generating the desired intermediate, which can be spectroscopically characterized either in a cryogenic matrix or in solution through fast kinetics studies. Moreover, the photochemical formation of intermediates may also have synthetic applications since this method is essentially independent of the experimental conditions and offers a great versatility; for example, the photochemical generation of carbenes is often advantageous with respect to thermal methods for synthetic purposes.^[1] However, several other potentially useful intermediates have been scarcely exploited. As an example, the phenyl cation has been characterized in matrix^[2] and in

the gas phase^[3] but is difficult to access in solution, the only general method being photolysis of diazonium salts,^[4] where care must be given to avoid competing radical paths.^[5] As a result, this cation has almost never been used as a synthetic intermediate.^[6] We have recently shown that the 4-aminophenyl cation **2** is efficiently generated by photoinduced heterolysis of the C–Cl bond in 4-chloroanilines^[7,8] (**1**, see Scheme 1) and this offers a smooth path for the arylation of alkenes, aromatics and heterocycles.^[9]



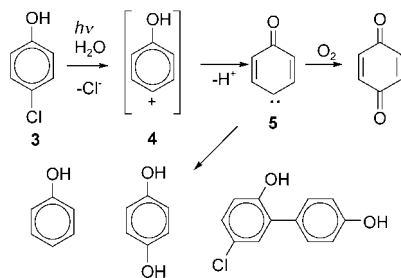
Scheme 1. Photoheterolysis of C–Cl bond in 4-chloroanilines according to ref. [7] and [8].

Apparently the interest of the reaction would increase if it could be extended to other haloaromatic compounds, at least to electron donating substituted derivatives. An obvious extension includes halophenols. In this case, there is substantial literature available, but no indication on a phenyl cation. In fact, the photochemistry of 4-chlorophenol

[a] Dr. I. Manet, Dr. S. Monti
Istituto ISOF-CNR, Area della Ricerca
Via Piero Gobetti 101, 40129 Bologna (Italy)
E-mail: monti@isof.cnr.it

[b] Dr. M. Fagnoni, Dr. S. Protti, Prof. Dr. A. Albini
Dipartimento di Chimica Organica
Università di Pavia, Viale Taramelli 10
27100 Pavia (Italy)
E-mail: angelo.albini@unipv.it

(3, Scheme 2) has been extensively studied, mainly in water, and it was found that chloride liberation is involved. In this case, the first intermediate characterized by flash photolysis has been 4-oxocyclohexa-2,5-dienylidene (5).^[10] This may



Scheme 2. Photochemistry of 4-chlorophenol in water according to ref. [10a].

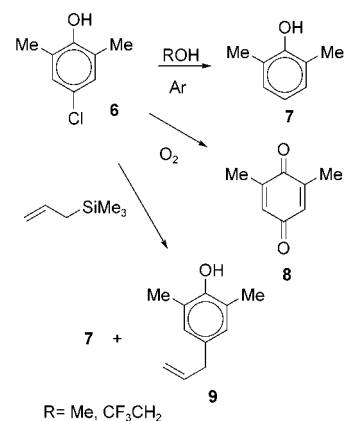
arise from the deprotonation of cation 4, but there is no evidence for this path. The role of 5 is supported by the formation of *p*-benzoquinone in the presence of oxygen. The processes occurring under anaerobic conditions, namely formation of hydroquinone, reduction to phenol (highly efficient in the presence of, or in neat, alcohols) and addition to the starting compound have been attributed to the same intermediate 5. With this rationalization, photolysis of halophenols appears to supplement photolysis of quinone monodiazo derivatives^[11] for the preparation of electrophilic carbenes such as 5.

Recently, however, unambiguous cationic arylations of arenes and of alkenes, similar to that observed for the aniline, have been reported for 4-chlorophenol.^[12] This suggested the intriguing question of whether fast deprotonation precludes obtaining a phenyl cation chemistry from halophenols, or both intermediates might have a role under suitable conditions and the intervention of highly reactive species such as cation 4 and carbene 5 could be discriminated and, in the event, controlled. If this were possible, the synthetic scope of the photochemical arylation could be assessed.

We decided to tackle this problem by product studies, diagnostic chemical trapping, steady state measurements and time-resolved studies. 2,6-Dimethyl-4-chlorophenol (6, Scheme 3) was chosen as the model compound in order to minimize self-addition to give dihydroxybiphenyl (compare Scheme 2). Since the key issue was whether deprotonation would inhibit reaction via the cation, the study was carried out in alcohols of different basicity (methanol and 2,2,2-trifluoroethanol) and the investigation was extended to the corresponding silyl ether, where an alternative O-linked electrofugal group was present.

Results

Products studies: The photochemical studies were carried out both on 1×10^{-3} M solutions with GC or HPLC periodical determination in order to monitor the course of the reaction as well as on more concentrated solutions (3 to 5×10^{-2} M)



Scheme 3. Photoproducts on irradiation of phenol 6 (for conditions see Experimental Section).

followed by chromatographic separation for the identification of the products. Irradiation of phenol 6 in argon-flushed methanol led to quantitative reductive dehalogenation and gave phenol 7 (Scheme 3). In oxygen-equilibrated methanol, however, phenol 7 was absent and 2,6-dimethyl-1,4-benzoquinone 8 was formed quantitatively in dilute solutions, although the yield was low at a higher concentration, probably due to polymerization.

The reaction was then carried out in the presence of a π -nucleophile. We chose an alkene rather than a benzene in order to facilitate selective irradiation (particularly for flash photolysis experiments, see below) and in particular allyltrimethylsilane (AS), because previous experience with related arylation reactions^[7,9a] showed that a single product (an allylbenzene) is obtained in this case. Indeed, when 6 was photolyzed in deoxygenated MeOH in the presence of growing amounts of AS, phenol 7 was gradually replaced by allylphenol 9, which became the main product at 0.2 M AS and was conveniently obtained by preparative irradiation in the presence of 1 M AS (Table 1). In preparative irradiation experiments with 5×10^{-2} M solutions of 6 allylphenol 9 was obtained as the main product also when omitting degassing.

The photochemistry of 6 was next examined in 2,2,2-trifluoroethanol (TFE) and gave a similar result, with reduction to phenol 7 and oxidation to quinone 8 in the absence and in the presence of oxygen, respectively (see Table 1). Furthermore, the allylated derivative 9 was largely dominating at 0.2 M AS. Preparative experiments in TFE led exclusively to 9 with 1 M AS, independently of the presence of oxygen.

In order to understand the role of the phenolic proton in the reaction, the photolysis of a silyl ether of the phenol was investigated. *tert*-Butyldimethylsilyl ether 10 (Scheme 4) was chosen since the corresponding trimethylsilyl ether was labile to traces of acids in methanol. The loss of the $t\text{BuMe}_2\text{-Si}^+$ cation from an intermediate during the above photoreactions would give compounds 7 to 9, that is, the same products obtained from phenol 6. This did, however, not occur. Irradiation in methanol under the same conditions as above led to two products, the silylated phenol 11, which resulted

Table 1. Photochemical reactions of phenol **6** and silyl ether **10**.

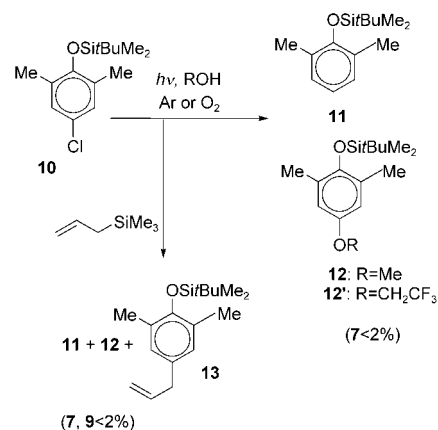
Reagent	Conditions	Products	Yield [%] ^[a]	
1×10^{-3} M solutions				
6	MeOH, Ar	7	85	
		8	<2	
	MeOH, O ₂	7	<2	
		8	86	
	MeOH, Ar, 0.2 M AS	7	40	
		9	48	
	TFE, Ar	7	85	
		8	<2	
	TFE, O ₂	7	92	
		8	7	
10	MeOH, Ar	11	40	
		12	48 ^[b]	
	MeOH, O ₂	11	13	
		12	5	
	MeOH, Ar, 0.2 M AS	11	4	
		12	tr	
		13	85 ^[b]	
	preparative experiments on 3.5×10^{-2} M solutions			
	6	MeOH, Ar	7	9
			9	52
TFE, Ar		9	70	
		11	18	
		12	tr	
	13	67		

[a] Calculations based on converted starting material, at 70–85% conversion. [b] A small amount of 2,6-dimethyl-4-fluorophenyl *tert*-butyldimethylsilyl ether was also present.

from reduction, and the 4-methoxy derivative **12**, likewise maintaining the silyl group, which resulted from formal solvolysis (Table 1). Only a trace amount of product **7** (<2%) was detected. In the presence of oxygen the reaction was slightly slowed, but no further product (e.g. quinone **8**) was formed. Likewise, irradiation in TFE gave **11** and the trifluoroethyl ether **12'**.

In the presence of AS, the silylated allylphenol **13** was formed at the expense of products **11** and **12** (or **12'**) in an amount depending on AS concentration in both methanol and TFE (Table 1 and Figure 1). Slightly negative intercepts in the linear plots of Figure 1 are reasonably due to experimental errors in the yield determinations at low AS concentrations. Product **13** was virtually free from the corresponding desilylated derivative **9** (<2%) (Scheme 4, Table 1). Irradiation of **10** in air equilibrated alcohols gives **11** and **12**, though the yield decreases at high conversion, apparently due to secondary decomposition. In the presence of AS the yield of **13** remains the same when omitting degassing.

Quantum yields and steady state competition: The fluorescence quantum yield was measured for compounds **6** and **10** and found to be in the order of 1% (see Table 2), independently of the solvent (e.g. for **6**, Φ_f 1.4, 0.9 and 0.8×10^{-2} in



Scheme 4. Photoproducts on irradiation of *tert*-butyldimethylsilyl ether **10** (for conditions see Experimental Section).

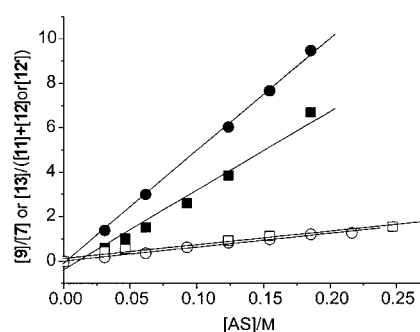


Figure 1. Ratio of the yield of product **9** vs that of product **7** in methanol (\circ) and in trifluoroethanol (\bullet). Ratio of the yield of product **13** versus the sum of the yields of products **11** and **12** (or **12'**) in methanol (\square) and in trifluoroethanol (\blacksquare).

cyclohexane, methanol and TFE, respectively). Low conversion experiments were also carried out to measure the quantum yield of the photodehalogenation reaction (Φ_r). The results are reported in Table 2 and show a modest effect of the presence of oxygen. The overall efficiency for the photolysis of both **6** and **10** was virtually unaffected by the presence of AS. In Figure 1, the ratio of the formation yield of allylphenol **9** to that of phenol **7** is plotted versus the AS concentration. A more steep dependence was observed in TFE than in MeOH. As for silyl ether **10**, the corresponding plot for the ratio of the yield of product **13** to the yield of the products formed in neat methanol (**11**+**12** or **12'**) is likewise reported in Figure 1.

Transient intermediates from 6 in TFE: Figure 2a shows the difference absorption spectrum obtained upon 266 nm laser flash photolysis of 1.5×10^{-3} M **6** in degassed TFE at 35 ns from pulse end (the shortest delay we were able to examine because of the fluorescence, see Experimental Section). This is characterized by a structured absorption with $\lambda_{\max} = 375/385$ nm (the more intense peak is underlined) and additional peaks at 290 and 250 nm. All the signals exhibited linear pulse energy dependence up to about 5 mJ per pulse (corre-

Table 2. Quantum yields and kinetic parameters for the reactions of phenol **6** and silyl ether **10**.

Reagent	Solvent	Φ_f	Φ_f ($\Phi_f^{O_2}$)	$k_{(9)}/k_{(7)}/M^{-1}$	k_0/s^{-1}	$k_{ad}/M^{-1}s^{-1}$	$k_{ad}/(k'_{ic}+k''_{ic}K_{eq})/M^{-1}$	$k_q^{O_2}/M^{-1}s^{-1}$
6	MeOH	9×10^{-3}	0.60 (0.48)	6	2.0×10^7	$\approx 1 \times 10^9$	≈ 10	3.0×10^9
6	TFE	8×10^{-3}	0.42 (0.40)	53	1.6×10^6	$\geq 2 \times 10^8$	125	3.6×10^9
10	MeOH	6×10^{-3}	0.29 (0.24)	6		$\approx 2 \times 10^8$		
10	TFE	6×10^{-3}	0.15	35				

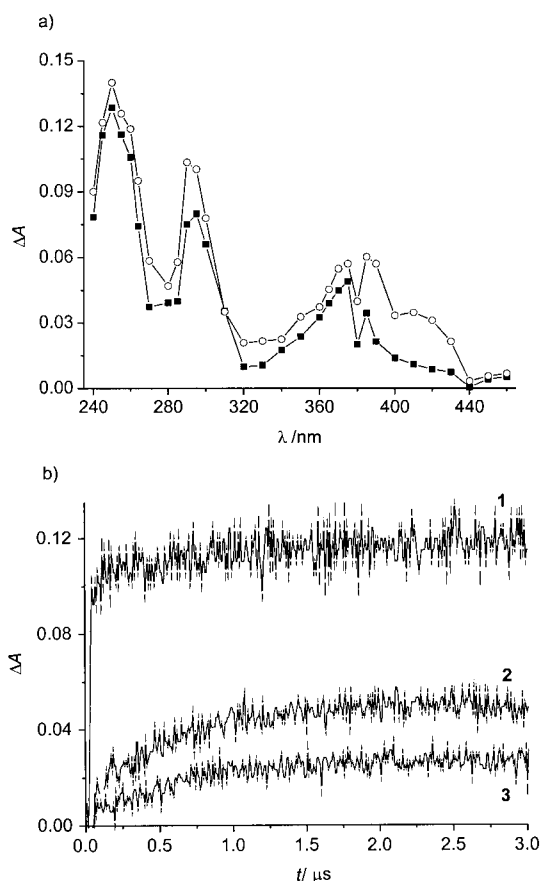


Figure 2. a) Difference absorption spectra of 1.5×10^{-3} M degassed TFE solution of **6** at (■) 35 ns and (○) 775 ns after pulse end. (3.5 mJ per pulse). b) Time course of ΔA at 1) 250 nm, 2) 390 nm, and 3) 420 nm (zero time at pulse onset).

sponding to 17 mJ cm^{-2}), in agreement with formation of the transients via a one photon mechanism.

The time evolution of the absorbance in the whole wavelength range was well described by a first-order kinetics with a time constant of 630 ± 60 ns and within this period, the first detected spectrum evolved to another one, rather similar in the UV but different in the near-visible region. It was characterized by peaks at $375/390$ nm and by an intense shoulder at $\lambda > 400$ nm. The same time constant was mea-

sured for the absorbance growing at 420, 250 and 390 nm (Figure 2b). On a longer time scale, the absorbance at 390 nm decayed biexponentially with $\tau_1 \sim 50 \mu\text{s}$ and $\tau_2 \sim 450 \mu\text{s}$. As for the transient at 420 nm, a lifetime $\tau \approx 250 \mu\text{s}$ could be estimated, but the absorbance did not decay completely, in part persisting in the millisecond time domain.

In the presence of AS, the difference spectrum at 30 ns from pulse end showed maxima at 250, 290 and $375/385$ nm and evolved with pseudo first order kinetics into an intense band at about 290–300 nm. With AS 0.045 M the time constant for the formation of the latter band was 90 ± 20 ns (see Figure 3a and b). The buildup rate of this band depended on the AS concentration according to Equation (1).

$$k_{\text{obs}} = k_0 + k_{\text{AS}} [\text{AS}] \quad (1)$$

A bimolecular rate constant $k_{\text{AS}} = (2 \pm 0.2) \times 10^8 \text{ M}^{-1} \text{ s}^{-1}$ with $k_0 = (1.3 \pm 0.5) \times 10^6 \text{ s}^{-1}$ could be estimated (see inset in Figure 3a). The absorbance decay measured at 320 nm was satisfactorily described by a biexponential function with time constants $\tau_1 = 30 \pm 2 \mu\text{s}$ and $\tau_2 = 150 \pm 10 \mu\text{s}$.

Photolysis of air-equilibrated TFE solutions of phenol **6** resulted in a difference absorption spectrum characterized by broad structured absorption with $\lambda_{\text{max}} = 430$ nm (Figure 4). This absorption band grew with pseudo first order kinetics with rate depending on the oxygen concentration. Thus, oxygen quenched a precursor characterized by $k_0 \sim (2.1 \pm 0.6) \times 10^6 \text{ s}^{-1}$ and a bimolecular rate constant $k_q^{O_2} = 3.6 \times 10^9 \text{ M}^{-1} \text{ s}^{-1}$ could be evaluated using an equation analogous to Equation (1) (see inset of Figure 4).

Transient intermediates from 6 in MeOH: Laser flash photolysis of Ar-flushed methanol solutions of **6** resulted in a difference spectrum exhibiting at 30 ns from pulse end two peaks of similar intensity at 375 and 390 nm, as well as intense bands at 250 and 290 nm (Figure 5). The time evolution of this transient was exponential with a time constant of about 50 ± 10 ns, essentially the same all over the spectrum, and led to a well defined spectrum with maxima at $375/390$ nm, 290 and 250 nm (see the spectral profile at ≈ 100 ns in Figure 5). The tail of the absorption at $\lambda > 400$ nm was weaker than in TFE. The decay of the transient at 390 nm was biexponential with $\tau_1 = 10 \pm 1 \mu\text{s}$ and $\tau_2 = 80 \pm 10 \mu\text{s}$.

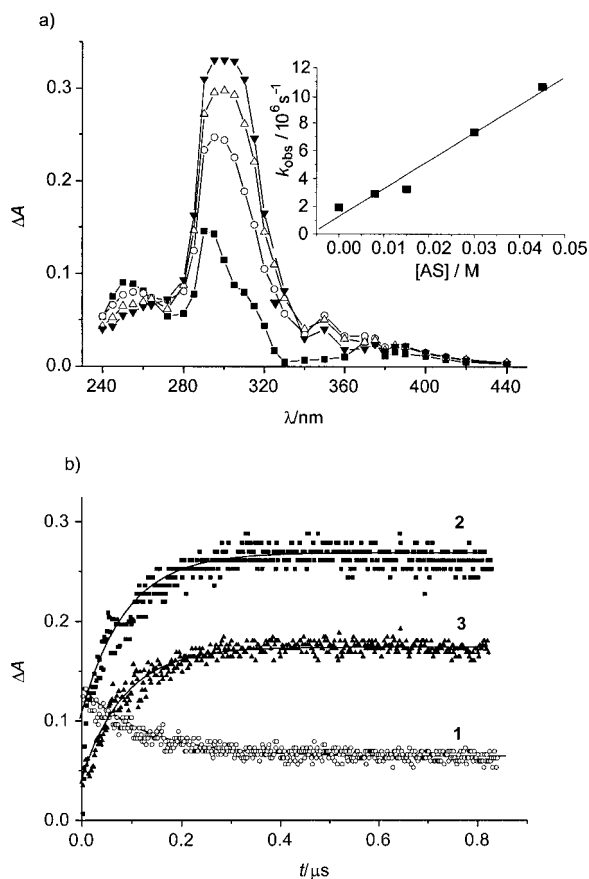


Figure 3. a) Difference absorption spectra of 1.5×10^{-3} M degassed TFE solution of **6** in presence of 0.045 M AS at (■) 35 ns, (○) 105 ns, (△) 180 ns, (▼) 780 ns from pulse end (4.0 mJ per pulse). Inset: Dependence of the build-up rate constant k_{obs} at 320 and 400 nm (in AS absence) on the AS concentration. b) Time course of ΔA at 1) 250 nm, 2) 290 nm, and 3) 320 nm (zero time at pulse end).

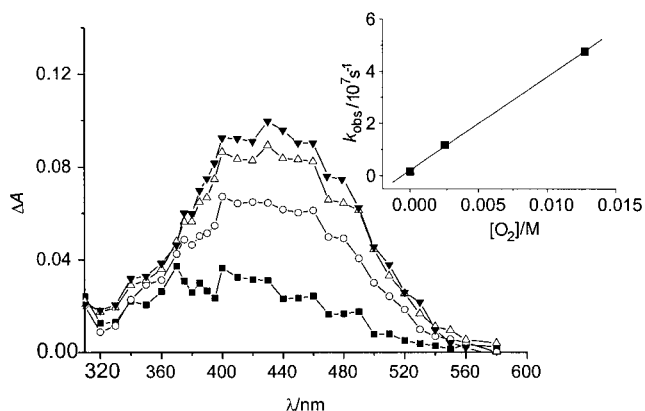


Figure 4. Difference absorption spectra from 1.5×10^{-3} M air-equilibrated TFE solution of **6** at (■) 30 ns, (○) 95 ns, (△) 180 ns, and (▼) 380 ns after pulse end (2.0 mJ per pulse). Inset: Dependence of the build-up rate constant k_{obs} at 460 and 390 nm (in oxygen absence) on the oxygen concentration.

In air-equilibrated methanol, an intense band at 490 nm was observed in addition to the 375/390 absorption

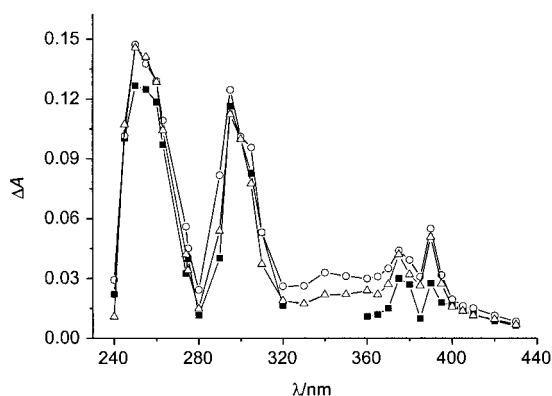


Figure 5. Difference absorption spectra of 1.4×10^{-3} M argon-flushed MeOH solution of **6** at (■) 30 ns, (○) 100 ns, and (△) 775 ns after pulse end (2.9 mJ per pulse).

(Figure 6). The buildup rate of both bands was the same in agreement with the reaction of a common precursor with molecular oxygen ($k_q^{O_2} = 3.0 \times 10^9 \text{ M}^{-1} \text{ s}^{-1}$, $k_0 = (1.8 \pm 0.6) \times 10^7 \text{ s}^{-1}$).

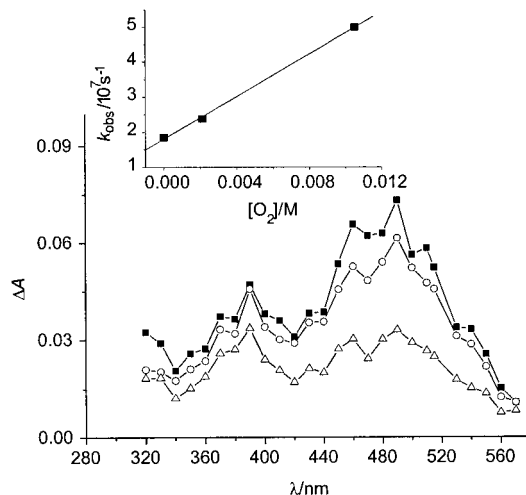


Figure 6. Difference absorption spectra of 1.4×10^{-3} M air-equilibrated MeOH solution of **6** at (■) 100 ns, (○) 480 ns, and (△) 1600 ns after pulse end (2.9 mJ per pulse). Inset: Dependence of the build-up rate constant k_{obs} at 460 nm and 390 nm (in oxygen absence) on the oxygen concentration.

The initial transient was quenched by AS also in MeOH, although the concentration of the additive required for observing a significant effect was larger than in TFE. This resulted in the buildup of a strong absorbance at 290 nm (compare the difference spectrum at 100 ns in Figure 7 with that in neat methanol in Figure 5), analogously to what observed in TFE. The bimolecular rate constant for the reaction with AS was approximately estimated from the buildup of the absorbance at 250 and 390 nm and found to be $k_{\text{AS}} \approx 2 \times 10^8 \text{ M}^{-1} \text{ s}^{-1}$. The decay of the transient at 390 nm was biexponential with $\tau_1 = 20 \pm 2 \mu\text{s}$ and $\tau_2 = 190 \pm 30 \mu\text{s}$ (see inset of Figure 7). At 320 nm a major fraction of the signal decayed with $\tau = 1.7 \mu\text{s}$, but a part persisted longer.

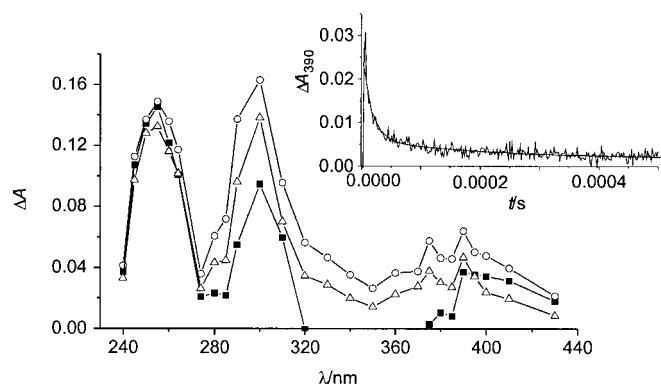


Figure 7. Difference absorption spectra of 1.4×10^{-3} M argon-flushed MeOH solution of **6** in presence of 0.1 M AS at (■) 30 ns, (○) 100 ns, and (△) 775 ns after pulse end (3.5 mJ per pulse). Inset: Biexponential decay of ΔA at 390 nm in 1 mm **6** in presence of 4.5×10^{-2} M AS in methanol.

Transient intermediates from 10 in MeOH: Laser photolysis of silyl ether **10** in Ar-flushed methanol (Figure 8a) resulted in a difference absorption spectrum characterized 10 ns after the laser pulse by bands at 260 and 360–390 nm. The spec-

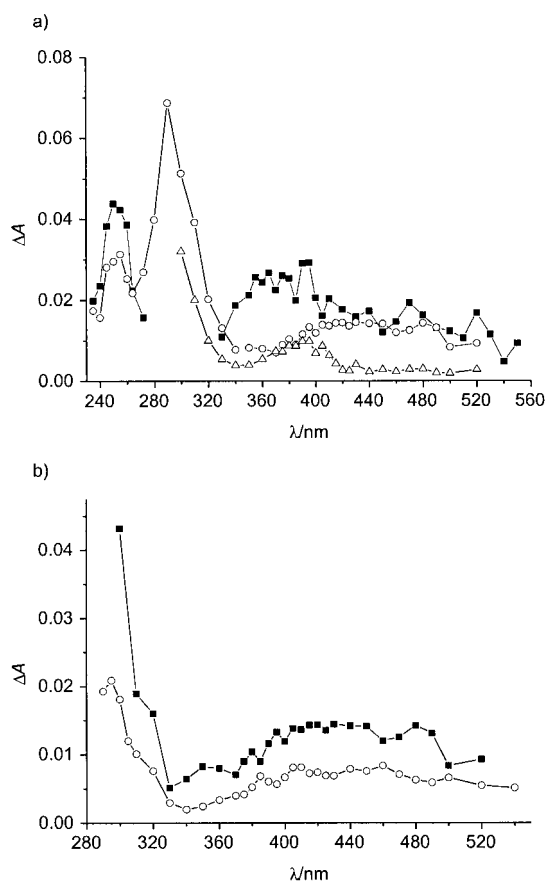


Figure 8. a) Difference absorption spectra of 1.4×10^{-3} M argon-flushed MeOH solution of **10** at (■) 10 ns, (○) 110 ns and (△) 1500 ns after pulse end (2.0 mJ per pulse). b) Difference absorption spectra of 1.4×10^{-3} M argon-flushed MeOH solution of **10** in the absence of AS (■) and in the presence of 0.25 M AS (○) at 110 ns after pulse end (2.0 mJ per pulse).

trum taken at ≈ 110 ns delay had well defined peaks at 255 and 290 nm and a broad band extending beyond 500 nm. The time evolution of the absorption changes was well described by a biexponential function with $\tau_1 \sim 22 \pm 5$ ns and $\tau_2 \sim 250 \pm 50$ ns. The surviving absorption (i.e., that at 1.5 μ s delay in Figure 8a) persisted in the millisecond range. The time constant τ_1 was slightly shorter in oxygen saturated solutions ($\tau_1^{O_2} \sim 15$ ns), but was not affected by the presence of 0.25 M AS. The time constant τ_2 was likewise unaffected by AS. On the contrary this additive strongly reduced the intensity of the visible absorption (Figure 8b). In Figure 9a the biphasic time course of the absorbance can be appreciated at 250 and 420 nm. In Figure 9b the effect of the presence of AS on the intensity of the longer lived component is shown at both wavelengths.

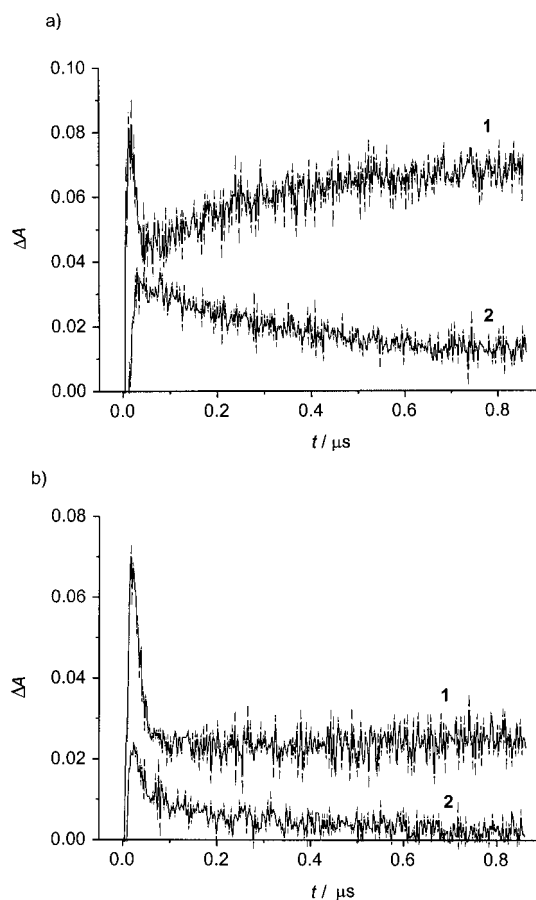
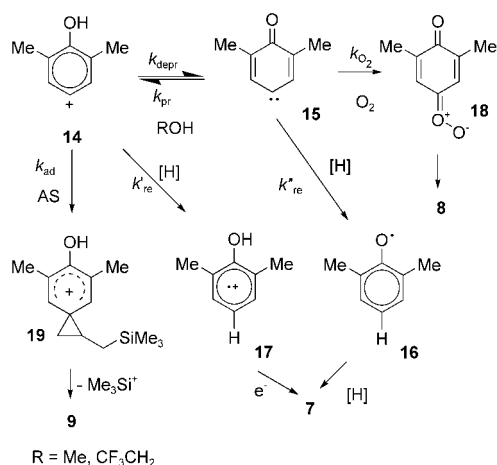


Figure 9. Time course of ΔA at 1) 255 nm and 2) 420 nm of 1.4×10^{-3} M argon-flushed MeOH solution of **10** a) in the absence of AS and b) in the presence of 0.25 M AS (2.7 mJ per pulse; zero time at pulse onset).

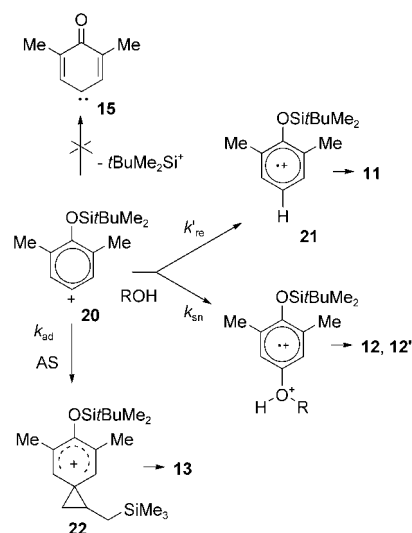
Discussion

Cation versus carbene: The aim of the present study is the identification and the evaluation of the synthetic utility of the intermediates generated by photolysis of 4-chlorophenol derivatives. Comparison of the photochemistry of com-

pounds **6** and **10** shows that both the reactions expected from triplet phenyl cation **14** and those expected from triplet carbene **15** are obtained in the presence of the appropriate traps (Schemes 5 and 6); for simplicity, **14** and **15** are indicated by a single formula, even if delocalization on the ring is important, see for example ref. [11k]). Indeed, allylphenol **9** is the product expected by addition of cation **14** to AS and subsequent elimination of the good electrofugal Me_3Si^+ group from adduct cation **19**. The reaction is closely analogous to that observed with chloroanilines, where addition followed by elimination of an electrofugal cation (H^+ , Me_3Si^+) have been characterized for a variety of π nucleophiles (alkenes, aromatics, heterocycles) and firmly rationalized as involving triplet aminophenyl cation **2**.^[9a] Formation of **9** via carbene **15** is not expected, since literature suggests that an isolable *spiro*-cyclopropanecyclohexadienone would rather be formed^[11] and such a hypothesis is finally discarded because the allylphenol **13** is obtained from **10** conserving the *tert*-butyldimethylsilyl group, and thus necessarily involving cation **22** (Scheme 6). Further, the benzoquinone **8** is a diagnostic trapping product of the carbene via carbonyl oxide **18** and is obtained from **6**, and not from **10** (see Table 1). Since the two observed reactions, with oxygen and with AS, cannot be imputed to a single intermediate, a convenient hypothesis is that cation and carbene are in equilibrium. As it will appear in the following, fast kinetic and steady state experiments support that kinetically indistinguishable intermediates are involved; indeed, the time resolved data obtained for **6** in both TFE and MeOH can be consistently rationalized assuming that the protonation equilibrium ($k_{\text{depr}}/k_{\text{pr}}$) between triplet aryl cation **14** and triplet carbene **15** is established within a few tens of nanoseconds, that is, with rates of the order of 10^8 s^{-1} . In the following, a structure assignment for the observed intermediates is presented and their role in the chemistry occurring discussed.



Scheme 5. Proposed mechanism of aryl cation evolution upon heterolytic photodehalogenation of **6**. For simplicity, mesomeric formulae of intermediates are not explicitly indicated.



Scheme 6. Proposed mechanism of aryl cation evolution upon heterolytic photodehalogenation of **10**. For simplicity, mesomeric formulae of intermediates are not explicitly indicated.

Assignment and role of transient species: Structure assignment for the transients observed under the various conditions is proposed on the basis of the analogy with previous studies and consistence with the mechanistic scheme discussed below.

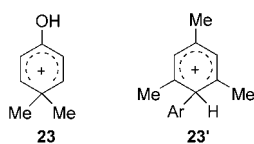
The fluorescence of phenol **6** hinders acquisition of meaningful signals before 30–35 ns from pulse end. In TFE, the first observed spectrum (Figure 2a) with maxima at 375/385, 290 and 250 nm is closely reminiscent of that attributed to triplet carbene **5** in water (Scheme 2).^[10a,11k] Recent computational investigations suggest that phenyl cations, except for particular substitution patterns, do not present intense absorption in the near UV or visible^[13] and thus cation **14** is not expected to contribute significantly in the spectral region explored. Thus, it seems reasonable to assign the earlier spectrum of Figure 2a to **15**. As hinted above, the time evolution of the absorbance changes in the whole wavelength range occurs with a single time constant (630 ns), requiring that interconversion between **14** and **15**—if any—occurs with rates significantly faster than that of the decay of these intermediates (Figure 2b). This time constant is relative to the *formation* of secondary intermediates, absorbing stronger than the precursor(s) in the explored range. Thus, the fact that the aryl cation does not contribute to the initial spectrum is irrelevant to the single exponential behavior of the system.

Actually, two secondary transients are formed with the same rate. Phenoxy radical **16** is identified by the distinctive peaks at 375/390 nm, apparent in the spectrum at 775 ns in Figure 2a that well fits what found with the non methylated analogue.^[14] This product results from hydrogen abstraction from the solvent by triplet carbene **15** (k'_{re} in Scheme 5). A shoulder at $\lambda > 400 \text{ nm}$ is apparent in the same spectrum, and is assigned to the radical cation **17**, arising from solvent hydrogen transfer to aryl cation **14** (k'_{re}). Radical cations

from phenols are indeed known to absorb in the 380–450 nm range^[15] and hydrogen transfer to the phenyl cation has been previously considered as an alternative mechanism for reduction of halophenols and haloanilines.^[7,10a] Final support for the assignment comes from the fact that a similar transient is observed with the silyl ether, where only this path is available for reduction (see below). The same intermediates are observed in MeOH, though **16** greatly predominates over **17** in this case (Figure 5).

In the presence of traps, the transients from **6** change in a way that closely matches the changes in product distribution (see Table 1). Thus, carbonyl oxide **18**, characterized by a strong absorption in the visible, dominates in the presence of oxygen and arises from trapping of **15** by oxygen (k_{O_2}), analogously to the case of **3**.^[10a,b] Actually, this intermediate has $\lambda_{\text{max}}=490$ nm in MeOH (Figure 6), 460 nm in water^[10a] and 430 nm in TFE (Figure 4). This parallels the ability of nucleophile assistance by these solvents,^[16] consistently with a not previously documented, but reasonable, increasing stabilization of this cumulene by nucleophilic solvents.

The conspicuous absorption change with $\lambda_{\text{max}}=290$ –300 nm observed in TFE in the presence of AS (Figure 3a) is attributed to formation of phenonium ion **19**. Such ions have been often invoked as intermediates, particularly in substitution reactions of phenethyl derivatives.^[17] There is no precedent in the literature available for a similar phenonium, but 1,1-dimethyl-4-hydroxybenzenium ion **23**, with a closely analogous structure, indeed absorbs at 295 nm (log ϵ 3.57 in both HClO₄ and H₂SO₄), supporting the attribution.^[18] Phenyl cations have been previously trapped by mesitylene yielding arylcyclohexadienyl cations (**23'**), which absorb strongly at 260 and 350 nm.^[4c] In methanol, observation of the AS effect requires a larger amount of the additive, but also in this case the intensity of the 290–300 nm band at 100 ns delay indicates that cation **19** has been formed, though to a lower extent than in TFE (Figure 7).



In the case of the silyl ether **10**, the difference spectrum could be registered after 10 ns. Under these conditions an early transient with absorption bands at 260 and 360–390 nm (Figure 8a) is detected. This is quenched by oxygen but not influenced by high concentrations of AS, and is identified as the triplet state ³**10**. The broad band in the visible (Figures 8 and 9) with a lifetime in the order of hundreds of nanoseconds is assigned to radical cation **21** (Scheme 6). This band is strongly decreased in the presence of 0.25 M AS (indeed, the visible part of the spectrum of the triplet is better evidenced under this condition); moreover its decay time is not changed in the presence of the alkene (see Figure 9a and b).

In this case, no absorption attributable to phenonium ion **22** is detected (see Figure 8b); apparently, this species is blue-shifted with respect to **19**.

Cation–carbene equilibrium and kinetics: The photochemistry of **6** in the two alcohols is thus essentially the same, with the difference that primary intermediates **14** and **15** decay at a much faster rate in MeOH, where the rate of reaction approaches that of interconversion, particularly when these species are trapped by some additive. In the simplified approach that equilibration between **14** and **15** is faster than their decay, the oxygen trapping reaction can be used to check the self-consistency of the rationalization in Scheme 5 (with [AS]=0), since carbonyl oxide **18** is conspicuously detected in both solvents. The kinetic equations are resolved in the dynamic equilibrium approximation, that is, with k_{depr} , $k_{\text{pr}} \gg k'_{\text{re}}, k''_{\text{re}}, k_{\text{O}_2}[\text{O}_2]$. Assuming the photodehalogenation occurs “instantaneously” from excited **6** with quantum yield Φ_r , the following equations apply, where superscript “0” indicates the value at $t=0$:

$$K_{\text{eq}} = \frac{k_{\text{depr}}}{k_{\text{pr}}} = \frac{[\mathbf{15}]^0}{[\mathbf{14}]^0} \quad (2)$$

$$[\mathbf{14}]^0 + [\mathbf{15}]^0 = \Phi_r[\mathbf{6}^*] \quad (3)$$

In the presence of oxygen k_{obs} is expressed by Equation (4):

$$k_{\text{obs}} = ((k'_{\text{re}} + k''_{\text{re}}K_{\text{eq}})/(1 + K_{\text{eq}})) + (k_{\text{O}_2}K_{\text{eq}}/(1 + K_{\text{eq}}))[\text{O}_2] \quad (4)$$

where $k_0 = (k'_{\text{re}} + k''_{\text{re}}K_{\text{eq}})/(1 + K_{\text{eq}})$ is the rate measured in the absence of oxygen and the experimental quenching rate constant $k_{\text{q}}^{\text{O}_2}$ by O₂ is represented by Equation (5):

$$k_{\text{q}}^{\text{O}_2} = k_{\text{O}_2}K_{\text{eq}}/(1 + K_{\text{eq}}) \quad (5)$$

When the reaction with oxygen is completed, the maximum concentration of carbonyl oxide **18** is expressed by Equation (6):

$$[\mathbf{18}]^{\text{max}} = k_{\text{O}_2}[\text{O}_2]K_{\text{eq}}[\mathbf{14}]^0/k_{\text{obs}} \quad (6)$$

In air-equilibrated solutions (Figures 4 and 6, $[\mathbf{6}^*] = 2.7 \times 10^{-5}$ M and 3.9×10^{-5} M, in TFE and MeOH, respectively), $[\mathbf{18}]^{\text{max}}$ can be calculated by using the dehalogenation quantum yields Φ_r of Table 2, the experimental bimolecular quenching rate constant $k_{\text{q}}^{\text{O}_2} = 3.6 \times 10^9$ and $3.0 \times 10^9 \text{ M}^{-1} \text{ s}^{-1}$ (Grabner et al. found $3.5 \times 10^9 \text{ M}^{-1} \text{ s}^{-1}$ for **4** in water),^[10a] the oxygen concentrations 2.55×10^{-3} M and 2.1×10^{-3} M, the observed decay rate constants $k_{\text{obs}} = 1.2 \times 10^7 \text{ s}^{-1}$ and $2.4 \times 10^7 \text{ s}^{-1}$ in TFE and MeOH, respectively. The calculated values of $[\mathbf{18}]^{\text{max}}$ are 7.8×10^{-6} M in TFE and 4.7×10^{-6} M in MeOH and the ratio compares well with the ratio of the respective experimental values of ΔA_{max} (0.10 and 0.07). This fact can be taken as an indication of the reliability of the ki-

netic model applied and of the validity of the dynamic equilibrium approximation. On the basis of the above calculations, the molar absorption coefficient ε_{\max} of **18** is predicted to be about 12800 and 14800 $\text{M}^{-1}\text{cm}^{-1}$ in TFE and MeOH, respectively, to be compared with the value of 9500 $\text{M}^{-1}\text{cm}^{-1}$ determined by Grabner for the analogous carbonyl oxide derived from **3** in water.^[10a]

Information about the position of the equilibrium in the two solvents can be obtained from k_0 (Table 2) with some assumption on the rates of the reductive processes. For the carbene derived from **3** in water, the rate constants for H abstraction from MeOH and EtOH were determined by Grabner to be $1 \times 10^6 \text{M}^{-1}\text{s}^{-1}$ and $6.4 \times 10^6 \text{M}^{-1}\text{s}^{-1}$, respectively.^[10a] Thus, for **15** in MeOH it can be assumed $k_{\text{re}}'' \sim [\text{MeOH}] \times 10^6 \text{s}^{-1}$. The literature suggests that α, α, α -trifluorination makes hydrogen transfer slower by at least one order of magnitude, as shown by the ≥ 10 times decrease in the rate coefficient for H-abstraction by the OH radical from TFE with respect to EtOH.^[19] Finally, k_{re}' can be assumed to be negligible in MeOH, as indicated by the fact that formation of radical cation **17** is a minor process in this solvent. With these hypotheses, K_{eq} turns out to be about 4 in MeOH and ≤ 0.2 in TFE ($T = 295 \text{K}$). This result is in agreement with the different basicity of the two alcohols^[16] that governs the rate of deprotonation of cation **14** to carbene **15** (k_{depr}) and the rate of the back reaction (k_{pr}).

The reservoir of the equilibrating primary intermediates is emptied in neat alcohols through the two channels leading to reductive dehalogenation. This has been monitored in different ways. First, transient absorption evidences that radical **16** is formed with a rate constant of 2×10^7 and $1.6 \times 10^6 \text{s}^{-1}$ in MeOH and TFE, respectively (Table 2). In principle, in TFE radical **16** could also result from the deprotonation of **17**, which is known to be fast.^[20] However, the transient spectra indicate that the two radicals are more likely formed in parallel. Second, the competition between reduction to phenol **7** and allylation to give **9** via **19** has been studied by steady state experiments in the presence of increasing amounts of AS. A linear dependence of the ratio $[\mathbf{9}]/[\mathbf{7}]$ on AS concentration according to Equation (7) has been found.

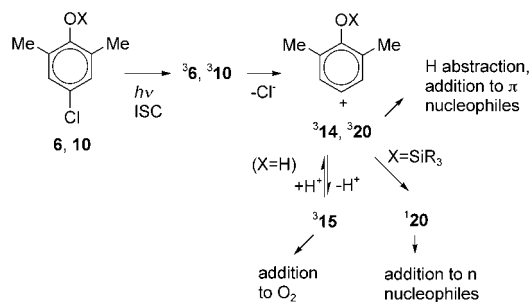
$$\frac{[\mathbf{9}]}{[\mathbf{7}]} = \frac{k_{(9)}}{k_{(7)}} [\text{AS}] \quad (7)$$

The linear plot in Figure 1 gave $k_{(9)}/k_{(7)} = 53 \text{M}^{-1}$ in TFE and 6M^{-1} in MeOH. Analogously, with silyl ether **10** the dependence of the $[\mathbf{13}]/([\mathbf{11}] + [\mathbf{12}])$ ratio on AS concentration gave $k_{(13)}/k_{(11+12)} = 35 \text{M}^{-1}$ in TFE and 6M^{-1} in MeOH. On the other hand, flash photolysis showed that the precursor of radical **17**, that is, $\mathbf{14} \rightleftharpoons \mathbf{15}$ is quenched by AS with rate constants $k_{\text{AS}} = 2 \times 10^8 \text{M}^{-1}\text{s}^{-1}$ in TFE and $\approx 2 \times 10^8 \text{M}^{-1}\text{s}^{-1}$ in MeOH. Within the equilibrium model assumed, $k_{\text{AS}} = k_{\text{ad}}/(1 + K_{\text{eq}})$ and $k_0 = (k_{\text{re}}' + k_{\text{re}}''K_{\text{eq}})/(1 + K_{\text{eq}})$; thus the ratio $k_{\text{ad}}/(k_{\text{re}}' + k_{\text{re}}''K_{\text{eq}})$ can be evaluated on the basis of the experimental values of k_0 ($1.6 \times 10^6 \text{s}^{-1}$ in TFE and $2.0 \times 10^7 \text{s}^{-1}$ in MeOH). The calculated ratios are $\approx 10 \text{M}^{-1}$ in MeOH and 125M^{-1} in TFE, showing a trend in reasonable agreement

with the $k_{(9)}/k_{(7)}$ values from the steady state experiments in the two solvents (see Table 2). As for the absolute value of k_{ad} , in MeOH it can be calculated by neglecting k_{re}' and using $k_{\text{re}}'' \sim [\text{MeOH}] \times 10^6 \text{s}^{-1}$ and the equilibrium constant of 4 and turns out to be about $10^9 \text{M}^{-1}\text{s}^{-1}$. In TFE a lower limit of $2 \times 10^8 \text{M}^{-1}\text{s}^{-1}$ is estimated.

In the case of silyl ether **10**, the only path available for reduction to **11** involves hydrogen transfer through radical cation **21**. The rate constant for the formation of the latter cannot be precisely measured due to the interference of the triplet absorption, longer lived than for **6**, but must be $k_{\text{re}} \geq 2.0 \times 10^7 \text{s}^{-1}$, on the basis of the observed ratio $k_{(13)}/k_{(11+12)} = 6 \text{M}^{-1}$, with addition to AS occurring with a rate constant $k_{\text{ad}} \sim 2 \times 10^8 \text{M}^{-1}\text{s}^{-1}$ also in this case.

Triplet versus singlet chemistry: Similarly to 4-chlorophenol,^[21] compound **6** shows a weak fluorescence (Φ_{f} ca. 1%) and an intersystem crossing quantum yield $\Phi_{\text{isc}} \geq 0.95$ is estimated; the same holds for compound **10**. Triplet $^3\mathbf{6}$ is not observed through transient absorption measurements in alcohols, although this should not be unduly stressed since, before 30 ns from pulse end, fluorescence perturbs detection of transient absorption signals, expected to be weak for triplet of phenol derivatives.^[14] In the case of **10** triplet absorption is observed and the short lifetime of 22 ns well fits with a dehalogenation reaction being an efficient decay channel (phenol and anisole have a lifetime of 3.3 μs in polar solvents).^[22] Furthermore, the similar photochemistry of **6** and **10** supports that the photoreaction is actually chloride loss in the triplet state, discarding the hypothesis that it involves concerted HCl elimination (Schemes 7 and 1).^[10a]



Scheme 7. Proposed mechanism of heterolytic photodehalogenation of **6** and **10**.

The rather efficient C–Cl bond cleavage thus proceeds from the triplet and, analogously to what happens with 4-chloroaniline, gives the corresponding phenyl cation in the triplet state. A difference between these two intermediates is that the triplet of 4-aminophenyl cation is markedly stabilized compared to the singlet ($\approx 10 \text{kcal mol}^{-1}$ according to B3LYP 6-31G(d) calculations), whereas the triplet of cation **14** is almost isoenergetic with the singlet (this latter is $\approx 1 \text{kcal mol}^{-1}$ more stable).^[23] In spite of this difference the

reactivity of the two intermediates is the same and proceeds in both cases from the triplet state. Inspection of the potential energy surfaces for triplet 4-aminophenyl cation showed that this adds easily to π , not to n , nucleophiles; with ethylene it gives a phenonium cation that intersystem crosses down to the singlet of the same structure.^[9a] Alcohols act as hydrogen donors to the triplet cation (and as O-nucleophiles to the singlet).^[4b,9a] We find here that, just like the amino analogue, cation **14** only gives addition to π nucleophiles and solvent induced reduction.^[24a] The cationic course of the reaction is supported by the formation of allylphenol **9** by loss of the trimethylsilyl cation from **19**, a largely precedented process with silanes when a cation, not a radical, is involved.^[24] It is worthwhile noting that Grabner found some hydroquinone from the irradiation of chlorophenol **3** in water (Scheme 2),^[10a] which could be an indication that in a non reducing medium triplet phenyl cation has no easy path available and ISC to the singlet has some role.

A further support to the above mechanism is offered by the chemistry of silyl ether **10**. First of all, this compound undergoes reductive dehalogenation to **11**, just as **6**, with no competing desilylation. Moreover, the involvement of transient **21** analogous to **17**, proves that a path for the reduction of the phenyl cation is operative not involving a carbene, that is, via the conversion **20**→**21**, analogously to **14**→**17**, not **14**→**15**→**16**. On the other hand, silyl ether **10** gives the methyl ether **12** in an amount comparable to that of the reduced compound **11**, through a reaction that is typical of *singlet* phenyl cation, and involves previous ISC from ³**20** to ¹**20**. Addition of AS inhibits both reactions to the same degree, indicating that effective trapping of the triplet cation successfully inhibits other decay paths from this intermediate.

Overall course of the reaction: The choice of the medium determines the course of the reaction after initial heterolytic cleavage of the C–Cl bond of phenol **6**. In methanol, proton transfer to nucleophilic MeOH is fast and the **14**⇌**15** equilibrium is shifted towards the latter species. This property, combined with the good hydrogen donor properties of this solvent makes the dehalogenation occur essentially via the carbene path as indicated for **3** by Grabner et al.^[10a] on the basis of flash photolysis data and further supported by CIDEP experiments (in 2-propanol).^[25] In more acidic TFE the equilibrium is shifted towards **14**. Additionally, this alcohol is a poor hydrogen donor and thus reduction to **7** is slow and for a large part occurs via the radical cation path. The two properties make this solvent better suited for trapping of the cation by a π nucleophile; thus, allylation by AS is largely predominant over reduction already at 0.1 M AS concentration. However, a high enough concentration of the alkene makes allylation successful even in MeOH, though this would clearly not be the solvent of choice for such reaction. Conversely, highly efficient O₂ trapping of **15** results in formation of the carbonyl oxide in both solvents, despite the different initial position of the equilibrium. When using a non deoxygenated 5×10⁻² M solution of **6**, the amount of

oxygen present is rapidly consumed and then the reaction continues undisturbed; thus, the photochemical preparation of allylphenol **9** can be carried out omitting degassing.

In the case of cation **20**, cleavage of the silyl cation is not sufficiently fast to be significant; therefore no **15** is formed and only reaction via the phenyl cation are observed. However, the difference in H donation between MeOH and TFE is well apparent, making trapping of the cation more effective in the latter solvent (compare Figure 1). A further difference with this cation is that ISC from the first formed triplet to singlet ¹**20**, reasonably the most stable state, occurs to some extent thus giving products **12** and **12'**, where the solvent act as n nucleophile, along with **11** (where it acts as H donor to ³**20**). However, addition of a π nucleophile syphons away ³**20** before ISC.

Conclusion

This work based on the comparison between a chlorophenol and the corresponding silyl ether strengthens the rationalization of the photochemical behavior of such compounds. The chemistry of **6** proceeds from the triplet and gives the hydroxyphenyl cation in the triplet state. This intermediate is not detected, nor is expected to be due to unfavorable absorption characteristics. However, this is unambiguously identified through trapping by an alkene leading to alkylation via a second intermediate, a phenonium ion. A transient corresponding to the last species is detected here for the first time, though such intermediates have been often invoked.^[17] In the protic solvents considered, a fast equilibrium between the hydroxyphenyl cation and triplet oxocyclohexadienylydene is established. Reactions both from the aryl cation (alkene addition and reduction) and the carbene (oxygen addition and reduction) have been characterized kinetically and the respective intermediates detected.

The mechanistic support obtained gives more confidence in synthetic applications. Triplet hydroxyphenyl cation is interesting from this point of view, due to the selective reaction with π nucleophiles, in particular with alkenes. The use of a less nucleophilic and, what is actually more important, less H-donating solvent such as TFE makes aryl cation chemistry accessible also at relatively low alkene concentration. This demonstrates that it is possible not only to discriminate, but also to direct the reaction. O-Silylation as in compound **10** is another way to obtain the aryl cation chemistry. In this case there is some incursion of singlet aryl cation chemistry in neat alcohols, which does not, however, decrease the efficiency of the arylation of alkenes.

The aryl cation chemistry previously obtained for 4-chloroanilines has been extended to a 4-chlorophenol derivative and its silyl ether, generalizing the photochemical method for the generation of aryl cations from electron-donating substituted haloaromatics. Indeed, phenyl cations are virtually inaccessible by thermal methods^[6] and their synthetic potential has not been appreciated as yet. Photochemistry may turn out to be the elective method in this case and may

give access to another class of reactions where a highly reactive intermediate is generated by irradiation under mild conditions.

Experimental Section

General: MeOH, TFE (Fluka) and allyltrimethylsilane (Lancaster) were used as received, 4-chloro-2,6-dimethylphenol (Lancaster) was purified by crystallization from cyclohexane. NMR spectra were measured in CDCl₃ with TMS as internal standard and accompanied by the appropriate DEPT experiments.

Preparation of 1-[(*tert*-butyldimethylsilyloxy]-2,6-dimethyl-4-chlorobenzene (10): The title compound was obtained in 90% yield and purified by bulb to bulb distillation starting from the corresponding phenol and by using the procedure reported by Aizpurua et al.^[26] Colorless solid, m.p. 28–30°C; elemental analysis calcd (%) for C₁₄H₂₃ClOSi: C 62.08, H 8.56; found: C 61.93, H 8.54; ¹H NMR (CDCl₃): δ = 0.2 (s, 6H), 1.1 (s, 9H), 2.2 (s, 6H), 6.95 (s, 2H); IR (neat): ν = 1470, 1224, 922, 854 cm⁻¹.

Preparation of 2,6-dimethyl-4-methoxyphenyl *tert*-butyldimethylsilyl ether (12) and 2,6-dimethyl-4-trifluoroethoxyphenyl *tert*-butyldimethylsilyl ether (12'): Authentic samples of these compounds for comparison with the photochemically obtained products were prepared from 2,6-dimethyl-4-methoxy- (or 4-trifluoroethoxy)-phenol. In turn, these were obtained from 2,6-dimethylhydroquinone, obtained by sodium dithionite reduction of 2,6-dimethyl-1,4-benzoquinone,^[27] followed by selective acid catalyzed methylation or, respectively, trifluoroethylation^[28] in the corresponding alcohols, by using the same procedure as above.

Compound **12**: colorless oil; elemental analysis calcd (%) for C₁₅H₂₆O₂Si: C 67.62, H 9.84; found: C 67.33, H 9.54; ¹H NMR (CDCl₃): δ = 0.2 (s, 6H), 1.0 (s, 9H), 2.2 (s, 6H), 3.75 (s, 3H), 6.55 (s, 2H); ¹³C NMR (CDCl₃): δ = 3.2 (CH₃), 18.6, 19.7 (CH₃), 26.0 (CH₃), 55.3 (CH₃), 113.6 (CH), 129.2, 145.7, 153.3; IR (neat): ν = 1485, 1436, 1253, 1222, 1068, 898, 838, 778 cm⁻¹.

Compound **12'**: colorless oil; elemental analysis calcd (%) for C₁₆H₂₅F₃O₂Si: C 57.46, H 7.53; found: C 57.10, H 7.80; ¹H NMR (CDCl₃): δ = 0.2 (s, 6H), 1.0 (s, 9H), 2.2 (s, 6H), 4.2 (q, 2H, J=8 Hz), 6.55 (s, 2H); IR (neat): ν = 1473, 1284, 1224, 1162, 1090, 905, 839, 779 cm⁻¹.

Photochemical reactions: 1 × 10⁻³ M or 5 × 10⁻² M solutions of either **6** or **10** in 1 cm diameter quartz tubes were flushed with argon for 15 min—when appropriate—, serum capped and irradiated at 295 K in a multi-lamp apparatus fitted with six 15 W phosphor coated lamps (centre of emission 310 nm). Conversion of the starting material and formation of the photoproducts were periodically monitored by GC or HPLC. The conversion was approximately linear up to >80% conversion. In the photoreaction of **10** in TFE a small amount of 2,6-dimethyl-4-fluorophenyl *tert*-butyldimethylsilyl ether was also formed, as indicated by GC/MS.

Photochemical synthesis of 2,6-dimethyl-4-(2-propenyl)phenol (9): The synthesis was carried out starting from 4-chloro-2,6-dimethylphenol **6** (82 mg, 0.52 mmol, 0.035 M), allyltrimethylsilane (2.4 mL, 15 mmol, 1 M) in MeOH (15 mL) were irradiated as above for 5.5 h at 310 nm. After column chromatography (cyclohexane/EtAc 98.5:1.5) the title compound was isolated as an oil (45 mg, 52%) along with 2,6-dimethylphenol (8 mg, 9%).

Compound **9**: colorless oil,^[29] elemental analysis calcd (%) for C₁₁H₁₄O: C 81.44, H 8.70; found: C 81.40, H 8.77; ¹H NMR (CDCl₃): δ = 2.25 (s, 6H), 3.30 (d, 2H, J=7 Hz), 4.55 (brs, 1H), 5.1 (m, 2H), 6.0 (m, 1H), 6.85 (s, 2H); IR (neat): ν = 3568, 1638, 1196 cm⁻¹.

Photochemical synthesis of 1-[(*tert*-butyldimethylsilyloxy]-2,6-dimethyl-4-(2-propenyl)benzene (13): From **10** (95 mg, 0.35 mmol, 0.035 M), allyltrimethylsilane (1.6 mL, 10 mmol, 1 M) and TEA (48.5 μL, 0.35 mmol, 0.035 M) in MeOH (10 mL) irradiated as above for 6 h. After column chromatography (cyclohexane), the title compound was isolated as an oil (65 mg, 67%) along with 1-[(*tert*-butyldimethylsilyloxy]-2,6-dimethylbenzene (**11**; 15 mg, 18%).

Compound **11**: colorless oil; ¹H NMR (CDCl₃): δ = 0.45 (s, 6H), 1.15 (s, 9H), 2.5 (s, 6H), 6.65 (t, 2H, J=7 Hz), 7.00 (d, 1H, J=7 Hz); further characteristics as reported.^[30] Data of compound **13** in accordance with literature.^[31]

Quantum yield measurement: The fluorescence quantum yields (Φ_f) in cyclohexane, methanol and trifluoroethanol were measured from the area of the corrected emission spectra (T=295 K, excitation at 285 nm) by using 9,10-diphenylanthracene as standard (Φ_f=0.91 in cyclohexane).^[32] Reaction quantum yields (Φ_r) were determined by irradiating 1 × 10⁻³ M solutions of either **6** or **10** in 1 cm optical path cuvettes after flushing with argon or oxygen. The lamp source was a focalized 150 W high pressure mercury arc fitted with an interference filter (transmission, 280 nm). Potassium ferrioxalate was used as the actinometer.

Nanosecond laser flash photolysis: The setup for the nanosecond absorption measurements was described previously.^[33] The minimum response time of the detection system was of about 2 ns. The laser beam (a JK-Lasers Nd/YAG operated at λ=266 nm, pulse FWHM 20 ns) was focused on a 3 mm high and 10 mm wide rectangular area of the cell and the first 2 mm in depth were analyzed at a right angle geometry. The incident pulse energies used were <17 mJ cm⁻² (5 mJ per pulse). The bandwidth used in the spectrokinetic measurements was typically 2 nm (0.5 mm slit width). The spectra were reconstructed point by point from time profiles taken each 5–10 nm. The sample absorbance at 266 nm was typically 1–1.5 over 1 cm. Oxygen was removed from methanol by vigorously bubbling the solutions with a constant flux of Ar, previously passed through an alcohol trap to prevent evaporation of the sample. The same procedure was used to prepare oxygen saturated solutions. The solution, in a flow cell of 1 cm path, was renewed after each laser shot. The TFE experiments and some methanol experiments were performed on samples degassed by repeated freeze-pump-thaw cycles at the vacuum line. In this case too, the solutions were renewed after a few laser shots. The temperature was 295 ± 2 K. The detector system was perturbed from 290 to 380 nm by the intense emission of **6**, generated by the laser excitation. These troubles were minimized by using neutral density filters at the entrance slit of the monochromator and pulsing the 150 W high pressure Xe lamp at high currents (~200 mA for 1 ms) to increase the intensity of the analyzing light. In spite of this, transient spectra in this wavelength region were not significant before 30–35 ns. Acquisition and processing of absorption signals were performed by a home made program using Asyst 3.1 (Software Technologies, Inc.). Nonlinear fitting procedures by the least square method and χ² and distribution of residuals were used to judge the goodness of the fit.

Acknowledgement

Partial support of this work by MIUR, Rome, is gratefully acknowledged.

- [1] a) *Carbenes* (Eds.: M. Jones, R. A. Moss), Wiley, New York, **1973**; b) H. Tomioka, *Photomed. Photobiol.* **1984**, *6*, 23.
- [2] a) H. B. Ambroz, T. J. Kemp, *J. Chem. Soc. Perkin Trans. 2* **1980**, 768; b) H. B. Ambroz, T. J. Kemp, G. K. Prybytniak, *J. Photochem. Photobiol. A* **1997**, *108*, 149; c) H. B. Ambroz, T. J. Kemp, *Chem. Soc. Rev.* **1979**, *8*, 353; d) M. Winkler, W. Sander, *Angew. Chem.* **2000**, *112*, 2091; *Angew. Chem. Int. Ed.* **2000**, *39*, 2014; e) A. Cox, T. J. Kemp, D. R. Payne, M. C. R. Symons, P. P. de Moira, *J. Am. Chem. Soc.* **1978**, *100*, 4779; f) H. B. Ambroz, T. J. Kemp, *J. Chem. Soc. Perkin Trans. 2* **1969**, 1420.
- [3] a) M. Speranza, *Chem. Rev.* **1993**, *93*, 2933; b) J. Hrusák, D. Schröder, S. Iwata, *J. Am. Chem. Soc.* **1993**, *115*, 2015; c) A. Filippi, G. Lilla, G. Occhiucci, C. Sparapani, O. Ursini, M. Speranza, *J. Org. Chem.* **1995**, *60*, 1250; d) M. Speranza in *Carbenes* (Eds.: M. Jones, R. A. Moss), Wiley, New York, **1973**, p. 157; e) N. E. Shchepina, V. D. Nefedov, M. A. Toropova, V. V. Avrorin, S. B. Lewis, B. Mattson, *Tetrahedron Lett.* **2000**, *41*, 5303.

- [4] a) H. Zollinger, *Diazochemistry I*, VCH, New York, **1995**; b) S. M. Gasper, C. Devadoss, G. B. Schuster, *J. Am. Chem. Soc.* **1995**, *117*, 5206; c) S. Steenken, M. Askokkuna, P. Maruthamuthu, R. A. McClelland, *J. Am. Chem. Soc.* **1998**, *120*, 11925; d) M. Milanese, M. Fagnoni, A. Albini, *Chem. Commun.* **2003**, 216.
- [5] a) C. Galli, *Chem. Rev.* **1988**, *88*, 565; b) T. M. Bockman, D. Kosynkin, J. K. Kochi, *J. Org. Chem.* **1997**, *62*, 5811.
- [6] a) P. J. Stang, in *Dicoordinated Carbocations* (Eds.: Z. Rappoport, P. J. Stang), Wiley, New York, **1997**, p. 451; b) M. Hanack, L. R. Subramanian, in *Methoden der Organischen Chemie (Houben-Weyl)*, Vol. E19C (Ed.: M. Hanack), Thieme, Stuttgart, **1990**, p. 249.
- [7] B. Guizzardi, M. Mella, M. Fagnoni, M. Freccero, A. Albini, *J. Org. Chem.* **2001**, *66*, 6353.
- [8] For further studies on the photochemistry of chloroanilines see a) K. Othmen, P. Boule, B. Szczepanik, K. Rotkiewicz, G. Grabner, *J. Phys. Chem. A* **2000**, *104*, 9525; b) B. Szczepanik, T. Latowski, *Pol. J. Chem.* **1997**, *71*, 807.
- [9] a) M. Mella, P. Coppo, B. Guizzardi, M. Fagnoni, M. Freccero, A. Albini, *J. Org. Chem.* **2001**, *66*, 6344; b) P. Coppo, M. Fagnoni, A. Albini, *Tetrahedron Lett.* **2001**, *42*, 4271; c) M. Fagnoni, M. Mella, A. Albini, *Org. Lett.* **1999**, *1*, 1299; d) B. Guizzardi, M. Mella, M. Fagnoni, A. Albini, *J. Org. Chem.* **2003**, *68*, 1067; e) B. Guizzardi, M. Mella, M. Fagnoni, A. Albini, *Tetrahedron* **2000**, *56*, 9383.
- [10] a) G. Grabner, C. Richard, G. Köhler, *J. Am. Chem. Soc.* **1994**, *116*, 11470; b) A. P. Y. Durand, R. G. Brown, D. Worrall, F. Wilkinson, *J. Chem. Soc. Perkin Trans. 2* **1998**, 365; c) A. P. Y. Durand, D. Brettan, R. G. Brown, *Chemosphere* **1992**, *25*, 723; d) A. P. Y. Durand, R. G. Brown, *Chemosphere* **1995**, *31*, 3595; e) A. P. Y. Durand, R. G. Brown, D. Worrell, F. Wilkinson, *J. Photochem. Photobiol. A* **1996**, *96*, 35; f) E. Lipzyska-Kochany, *Chemosphere* **1992**, *24*, 911; g) F. Bonnichon, G. Grabner, G. Guyot, C. Richard, *J. Chem. Soc. Perkin Trans. 2* **1999**, 1203; h) B. R. Arnold, J. C. Scaiano, G. F. Bucher, W. Sander, *J. Org. Chem.* **1992**, *57*, 6469.
- [11] a) W. Sander, C. Köttinger, W. Hubert, *J. Phys. Org. Chem.* **2000**, *13*, 581; b) W. Sander, R. Hubert, E. Kraka, J. Grafenstein, D. Cremer, *Chem. Eur. J.* **2000**, *6*, 4567; c) H. H. Wenk, R. Hubert, W. Sander, *J. Org. Chem.* **2001**, *66*, 7994; d) W. Sander, H. F. Bettinger, *Adv. Carbene Chem.* **2001**, *3*, 159; e) V. V. Ershov, G. A. Nikiforov, C. R. de Jonge, *Quinone Diazides*, Elsevier, Amsterdam, **1981**; f) K. W. Field, G. B. Schuster, *J. Org. Chem.* **1988**, *53*, 4000; g) T. Ohno, N. Martin, B. Knight, F. Wudl, T. Suzuki, H. Yu, *J. Org. Chem.* **1996**, *61*, 1306; h) M. Lahrech, S. Hacini, J. L. Parrain, M. Santelli, *Tetrahedron Lett.* **1997**, *38*, 3395; i) C. Kötting, W. Sander, *J. Am. Chem. Soc.* **1999**, *121*, 8891; j) H. D. Becker, T. Elebring, *J. Org. Chem.* **1985**, *50*, 1319; k) carbene **15** has been characterized in Ar matrix, see G. Bucher, W. Sander, *J. Org. Chem.* **1992**, *57*, 1346.
- [12] S. Protti, M. Fagnoni, M. Mella, A. Albini, *J. Org. Chem.* **2004**, *69*, 3465.
- [13] D. M. Smith, Z. B. Maksic, H. Maskill, *J. Chem. Soc. Perkin Trans. 2* **2002**, 906.
- [14] G. Grabner, G. Köhler, S. Marconi, S. Monti, S. Venuti, *J. Phys. Chem.* **1990**, *94*, 3609.
- [15] a) V. E. Zubarev, O. Brede, *Acta Chem. Scand.* **1997**, *51*, 224; b) T. A. Gadosy, D. Shukla, L. J. Johnston, *J. Phys. Chem. A* **1999**, *103*, 8834; c) M. R. Ganapathi, S. Naumov, R. Hermann, O. Brede, *Chem. Phys. Lett.* **2001**, *337*, 335.
- [16] a) T. W. Bentley, C. T. Bowen, D. H. Morten, P. v. R. Schleyer, *J. Am. Chem. Soc.* **1981**, *103*, 5466; b) T. W. Bentley, G. E. Carter, *J. Am. Chem. Soc.* **1982**, *104*, 5741; c) T. W. Bentley, G. E. Carter, H. C. Harris, *J. Chem. Soc. Chem. Commun.* **1984**, 387; d) R. Tashma, W. P. Jenks, *J. Am. Chem. Soc.* **1986**, *108*, 8050.
- [17] A. Asensio, J. J. Dannenberg, *J. Org. Chem.* **2001**, *66*, 5996 and references therein.
- [18] V. P. Vitullo, *J. Org. Chem.* **1970**, *35*, 3976.
- [19] a) K. Tokuhashi, H. Nagai, A. Takahashi, M. Kaise, S. Kondo, A. Sekiya, M. Takahashi, Y. Gotoh, A. Suga, *J. Phys. Chem. A* **1999**, *103*, 2664; b) R. Atkinson, D. L. Baulch, R. A. Cox, R. F. Hampson, J. A. Kerr, J. Troe, *J. Phys. Chem. Ref. Data* **1989**, *18*, 881.
- [20] a) F. G. Bordwell, J. Chen, *J. Am. Chem. Soc.* **1991**, *113*, 1736; b) S. Re, Y. Osamura, *J. Phys. Chem. A* **1998**, *102*, 3798; c) C. Trindle, *J. Phys. Chem. A* **2000**, *104*, 5298; d) D. M. Holton, D. Murphy, *J. Chem. Soc. Faraday Trans. 2* **1979**, 1637.
- [21] a) B. Koutek, L. Musil, I. Velek, M. Soucek, *Collect. Czech. Chem. Commun.* **1985**, *50*, 1753; b) P. Boule, C. Guyot, J. Lemaire, *Chemosphere* **1982**, *11*, 1179.
- [22] D. V. Bent, E. Hayon, *J. Am. Chem. Soc.* **1975**, *97*, 2599.
- [23] M. Aschi, J. N. Harvey, *J. Chem. Soc. Perkin Trans. 2* **1999**, 1059.
- [24] a) On the contrary, both the singlet phenyl cation (ref. [4b,d]) and the singlet oxocyclohexadienyldene (ref. [24b]) give ethers with alcohols; b) W. Kirmse, R. Legelmann, K. Friedrich, *Chem. Ber.* **1991**, *124*, 1853; c) W. P. Weber, in *Silicon Reagents for Organic Synthesis*, Springer, **1983**.
- [25] A. Ouardoui, C. A. Steren, H. van Willigen, C. Yang, *J. Am. Chem. Soc.* **1995**, *117*, 6803.
- [26] J. M. Aizpurua, C. Palomo, *Tetrahedron Lett.* **1985**, *26*, 475.
- [27] L. A. Carpino, S. A. Triolo, R. D. Berglund, *J. Org. Chem.* **1989**, *54*, 3303.
- [28] M. Greutar, H. Schmid, *Helv. Chim. Acta* **1972**, *55*, 2382.
- [29] J. B. Baruah, *Tetrahedron Lett.* **1995**, *36*, 8509.
- [30] R. E. Donaldson, P. L. Fuchs, *J. Org. Chem.* **1977**, *42*, 2032.
- [31] S. R. Angle, D. O. Arnaiz, J. P. Boyce, R. P. Frutos, M. S. Louie, H. L. Mattson-Arnaiz, J. D. Rainier, K. D. Turnbull, W. Yang, *J. Org. Chem.* **1994**, *59*, 6322.
- [32] S. R. Meech, D. Phillips, *J. Photochem.* **1983**, *23*, 193.
- [33] S. Monti, N. Camaioni, P. Bortolus, *Photochem. Photobiol.* **1991**, *54*, 577.

Received: July 5, 2004
Published online: November 12, 2004